Journal of Taibah University Medical Sciences (2024) 19(1), 198–208

Taibah University

Journal of Taibah University Medical Sciences

www.sciencedirect.com

Original Article

Speckle tracking echocardiography for diagnosis of right ventricular failure in children with totally corrected tetralogy of Fallot in Sulaimani, Iraq

Niaz M. Kamal, Ph.D. [a,*], Aso F. Salih, MBChB, DCHFIBMS [b] and Bushra M. Ali, FICMS [c]

[a] Pediatrics Department, Technical Institute, Sulaimani Polytechnic University, Sulaymaniyah, Iraq
[b] Pediatrics Department, Medicine College, University of Sulaimani, Sulaymaniyah, Iraq
[c] Family and Community Medicine Department, Medicine College, University of Sulaimani, Sulaymaniyah, Iraq

Received 5 July 2023; revised 21 September 2023; accepted 9 November 2023; Available online 22 November 2023

الملخص

أهداف البحث: هدفت الدراسة إلى استخدام "تخطيط صدى القلب بتتبع البقع" كتقنية جديدة لتشخيص فشل البطين الأيمن لدى الأطفال مع التصحيح الكامل لجراحة رباعية فالوت.

طريقة البحث: أجريت دراسة شبه تجريبية في مستشفى قلب الأطفال والمستشفى عالي الجودة في السليمانية لمدة تسعة أشهر. تم تسجيل 150 طفلا تتراوح أعمارهم بين 3 و13 عاما في حالة رباعية فالوت التي تم إصلاحها بالكامل للتحقيق في حمى الوادي المتصدع. تم تقدير حجم العينة اعتمادا على معدل انتشار رباعية فالوت بنسبة 7% إلى 10% من مجمل أمراض القلب التاجية. قياسات تخطيط صدى القلب التقليدية، بما في ذلك الكسر القذفي للبطين الأيمن، والانحراف الانقباضي للمستوى الحلقي ثلاثي الشرفات، ومؤشر أداء عضلة القلب، وحجم البطين الأيمن الانقباضي والانبساطي. بالإضافة إلى ذلك، تتبع البقع للإجهاد الإقليمي والطولي ومعدل الإجهاد في المنظر القمي المكون من 4 غرف. يتضمن تشخيص حمى الوادي المتصدع تخطيط كهربية القلب لقياس ثلاث عوامل: تشتت الموجة "بي"، وتشتت الموجة "تي"، ومدة "كيو آر اس".

النتائج: أظهر الأطفال الذين تم إصلاح رباعية فالوت والذين تم تشخيص إصابتهم بحمى الوادي المتصدع من خلال تخطيط صدى القلب التقليدي انحرافا انقباضيا غير طبيعي في المستوى الحلقي ثلاثي الشرفات قدره 1.3 ± 0.11 سم، وجزء القذف البطيني الأيمن 35.5 ± 6.72، ونهاية انقباضية للبطين الأيمن 69.8 ± 15.13 مل، ونهاية انقباضية والحجم الانبساطي 110.1 ± 14.13 مل، مؤشر أداء عضلة القلب 0.60 ± 0.12 ، و أقصى ضغط لجهاز التنفس الصناعي 52.4 ± 14.08. مقارنة بالأطفال ذوي وظيفة البطين الأيمن الطبيعية. كشف تطبيق تتبع البقع في تشخيص حمى الوادي المتصدع عن انخفاض معدل الإجهاد والإجهاد الطولي (-12.1 ± 2.3 و-0.9 ± 0.3) في الأطفال المصابين بحمى الوادي المتصدع. علاوة على ذلك، كانت هناك ارتباطات إيجابية ملحوظة بين سلالة البطين الأيمن الطولية والانحراف الانقباضي للمستوى الحلقي ثلاثي الشرفات (ص = 0.656) وكذلك الكسر القذفي (ص = 0.675) بينما تظهر الارتباطات السلبية مع حجم البطين الأيمن الانبساطي (ص = -0.684)، حجم نهاية الانقباضي للبطين الأيمن (ص = -0.718)، مؤشر أداء عضلة القلب (ص = -0.735)، و أقصى ضغط لجهاز التنفس الصناعي (ص = -0.767).

الاستنتاجات: يعد تطبيق تتبع البقع مع "معدل الإجهاد والانفعال" البطيني الأيمن الطولي لتقدير وظيفة البطين الأيمن في رباعية فالوت التي تم إصلاحها طريقة جديدة ومتقدمة تعمل على تحسين تشخيص تشوهات عضلة القلب الإقليمية وسرعة حركة عضلة القلب بشكل كبير مقارنة بالصدى التقليدي.

الكلمات المفتاحية: فشل البطين الأيمن؛ تتبع البقع؛ الكسر القذفي؛ رباعية فالوت؛ تخطيط صدى القلب؛ الإجهاد

Abstract

Objectives: The study was aimed at using speckle tracking echocardiography as a novel technique to diagnose right ventricular failure (RVF) in children with total correction of tetralogy of Fallot (TOF) through surgery.

Methods: A quasi-experimental study was performed at the Children's Heart Hospital of Sulaimani for 9 months. A total of 150 children with completely repaired TOF were enrolled to investigate RVF. Conventional echocardiographic data were recorded, including right ventricular (RV) ejection fraction (EF), tricuspid annular

* Corresponding address: Pediatrics Department, Technical Institute, Sulaimani Polytechnic University, Sulaymaniyah, Iraq.
E-mail: niaz.kamal@spu.edu.iq (N.M. Kamal)
Peer review under responsibility of Taibah University.

Production and hosting by Elsevier

1658-3612 https://doi.org/10.1016/j.jtumed.2023.11.005

plane systolic excursion (TAPSE), myocardial performance index (MPI), and RV end-systolic and diastolic volume (RVESV and RVEDV). Additionally, speckle tracking was performed for the regional and longitudinal strain and strain rate in four-chamber apical view. RVF diagnosis was determined on the basis of electrocardiography measurement of P-wave dispersion, T-wave dispersion, and QRS duration.

Results: Children with repaired TOF who were diagnosed with RVF through conventional echocardiography exhibited abnormalities with respect to children with normal RV function, including a TAPSE of 1.3 ± 0.11 cm, RVEF of 35.5 ± 6.72, RVESV of 69.8 ± 15.13 ml, RVEDV of 110.1 ± 14.13 ml, MPI of 0.60 ± 0.12, and Pmax of 52.4 ± 14.08. The use of speckle tracking in RVF diagnosis revealed a relatively lower longitudinal strain and strain rate (−12.1 ± 2.3 and −0.9 ± 0.3, respectively) in the children with RVF. Moreover, longitudinal right ventricular strain was positively correlated with TAPSE (r = 0.656) and EF (r = 0.675), and negatively correlated with RVEDV (r = −0.684), RVESV (r = −0.718), MPI (r = −0.735), and Pmax (r = −0.767).

Conclusions: The application of speckle tracking with the longitudinal RV strain and strain rate to estimate RV function in children with repaired TOF is a new advanced method that, compared with conventional echo, significantly improves the diagnosis of regional myocardial deformations and cardiac muscle motion velocity.

Keywords: Echocardiography; Ejection fraction; Right ventricular failure; Speckle tracking; Strain; TOF

Introduction

Tetralogy of Fallot (TOF), a type of CHD, is the most complex and common cyanotic cardiac malformation in patients older than neonatal age. The prevalence of TOF is approximately 7−10% of all congenital heart diseases. TOF is classified into two types: blue TOF and pink TOF, which affect boys and girls equally.[1] The CHD recognized as TOF was initially described by Niels Stensen in Denmark in 1671.[2] TOF manifests as a combination of four cardiac deformities: pulmonary artery narrowing, a hole in the ventricular septum, displacement of the aorta, and right ventricular (RV) hypertrophy.[3] With advances in medical technology, such as fetal echocardiography (ECG), TOF can be diagnosed during pregnancy at 12−15 weeks. TOF is typically diagnosed in early infancy, on the basis of a loud murmur or cyanosis, or ECG data.[4,5] In general, the treatment of TOF depends on the severity and type of subpulmonary obstruction, and surgery is the only effective treatment for TOF. In 1955, total correction of TOF was initially introduced and included intracardiac repair; this method is now used worldwide. The initial TOF repairs involved placement of a patch in the RV outflow tract through the annulus to alleviate the blockage. According to a literature review, approximately 10% of patients develop complications such as pulmonary regurgitation after TOF correction surgery and consequently require intervention.

Furthermore, prolonged PR can lead to chronic volume overload in the RV, thereby resulting in RVF, arrhythmias, and unfavorable cardiovascular outcomes.[6] RVF is common in corrected TOF cases and is believed to be significantly associated with heart failure morbidity and mortality.[7] Consequently, early diagnosis of RV function is useful for eliminating risk in patients with heart failure, guiding clinicians in the best treatment choice, and improving patient prognosis.[8,9] Assessing the function of the right ventricle in patients with repaired TOF (rTOF) with ECG is difficult because of the intricate crescent shaped RV.[10] Speckle tracking echo is a reliable method for investigating ventricular function. RV strain obtained through STE is a sensitive parameter that plays a crucial role in evaluating RV function and has prognostic value in RVF, because of its ability to detect early stage subclinical dysfunction.[11,12] The categorization of RV strain is based on the direction of myocardial movement and includes three types: RV longitudinal strain (RVLS), circumferential strain, and radial strain.[13,14] The assessment of diminished RVLS has significant prognostic value in various cardiovascular diseases, particularly in early stages of RV systolic dysfunction.[15,16] The novel method of documenting myocardial motion provides a non-invasive approach to assess vectors and velocity. The process involves automated tracking of myocardial deformation by using 2D or 3D speckle-tracking imaging. This technique allows for offline analysis of ST and SR to evaluate RV myocardial deformation and function.[17,18] STE is an advanced no-risk and low-cost method for RVF diagnosis in patients, commonly with TOF correction. Several studies have shown that the duration of the QRS complex serves as an indicator for evaluating RV function in patients who have undergone rTOF. Patients with rTOF commonly experience RV dysfunction and an extended QRS duration.[19,20] In patients without underlying heart disease, prolonged P-wave duration and increased P dispersion have been associated with an elevated risk of developing atrial fibrillation.[21] This study was aimed at investigating the diagnostic potential of speckle tracking, particularly strain and strain rate, for identifying RV failure in children with total correction of TOF.

Materials and Methods

Sample size and setting

This quasi-experimental study was performed at the Children's Heart Hospital of Sulaimani from October 1, 2021, to June 1, 2022. Children's Heart Hospital, situated in the heart of Sulaymaniyah City, is the largest hospital specializing in the comprehensive care of children with CHD and other cardiac conditions. It offers a wide range of services, including diagnosis, catheterization interventions, and open-heart surgeries. With its busy daily schedule, the hospital is dedicated to diagnosing and treating many children with CHD, and providing them with the necessary follow-up and care. To investigate RVF, this study included 150 children with a status of rTOF. The sample size was estimated according to a prevalence of TOF of 7−10% of all CHD. All children with rTOF underwent conventional and speckle-tracking ECG studies performed by the same pediatric cardiologist. Data for diagnosis of RV function were obtained prospectively from echo, and extracted to a data extraction form.

Inclusion criteria

The study population comprised children 3−13 years of age with complete TOF repair, who were residents of Sulaimani province.

Exclusion criteria

Children with Blalock-Taussig shunt, and children who were diagnosed with TOF but did not undergo surgery, were excluded. Children with rTOF were diagnosed with RVF. Children with an interval of less than 1 year between surgery and follow-up were excluded.

Echocardiography measurement and procedure

ECG was performed with a model Vivid E9 cardiovascular ultrasound system (a Phillips echo machine with four probes using an Sc-D multifrequency transducer) to investigate RVF in rTOF children. Three methods were used: two-dimensional (2D) tissue Doppler (TDI), and speckle tracking strain and strain rate. The patients were examined in dorsal supine position or left lateral decubitus in the conventional parasternal view, long and short axis view, four-chamber apical view, and subcostal view (subxiphoid). Subsequently, routing diagnostic imaging, including 2D echo and continuous-wave TDI apical recording, was obtained, and all examinations were recorded for offline analysis. In AP4-RV view, all parameters associated with the right chamber were examined, except the RV outflow tract dimension, and were measured in the parasternal short-axis view. RV systolic function was evaluated with conventional non-volumetric parameters commonly recommended in clinical practice. All RV function parameters were collected according to American Society of ECG guidelines for evaluating right heart function.[22] Subsequently, 2DE was used to assess RVEDV, RVESV, tricuspid annular plane systolic excursion (TAPSE), and EF, by using Simpson methods and global RV function. Pulse Doppler for a measure of tie index or MPI for RV function and pulmonary gradient. Any children examined by echo who had an abnormal ejection fraction (EF) < 45%, TAPSE <17 cm, and longitudinal RV strain <15% were considered to have RVF.[23,24]

Echocardiography speckle tracking measurement

All patients underwent STE in apical view. RV function was assessed by calculation of RVS and SR with a modified apical four chamber view. The 2D longitudinal strain analysis frame rates ranged from 40 to 80 frames per second. To evaluate the regional ST and SR of the RV, we delineated the endocardium and myocardium of the RV as three segments, near the annulus, middle, and apex of the free wall. A heartbeat with maximum image quality was selected for analysis, and the assessed RV measurements included longitudinal strain (LS) and SR. In addition, ECG with three leads was used; two leads were placed on the right shoulder and left shoulder, whereas the N lead was positioned on the left leg. The RV wall was then manually delineated in AP4-RV view, thus creating a region of interest during the QRS complex duration during peak systole. In healthy individuals, the RV base lateral strain generally exhibits values ranging from −20% to −30%. The mid-lateral strain typically ranges from −15% to −25%, whereas the apex lateral strain is commonly observed to be between −10% and −20%. The normal longitudinal strain rate of the RV base segment is typically between −1.0 and −2.0. The mid-segment strain rate ranges from −1.5 to −2.5, and the apex-segment strain rate ranges from −1.0 to −2.0.[25]

Electrocardiography

All children were examined with ECG at rest in a dorsal supine position. The tenth lead was used with six chests and four extremities. Two ECG speeds were performed for each patient, with an ECG paper speed of 25 and 50 mm/s for evaluation of T wave dispersion (T-WD), and P wave dispersion (P-WD). The P-WD was determined by subtraction of the longest and shortest P-wave durations among the ten ECG leads, with an ECG paper speed of 50 mm/s. TW-D was determined by evaluation of the T waves in leads V4, V5, and V6, because these leads typically exhibit upright T wave morphology. The T-wave was identified by measurement of the interval between the J point and the T offset in each lead of the ECG paper with a speed of 50 mm/s. QRS duration was measured from leads V4, V5, and V6 (maximum value) from the start of the Q wave to the completion of the S wave, with an ECG paper speed of 25 mm/s.

Statistical analysis

The analysis was conducted in Stata version 14. All categorical variables are expressed as frequencies and percentages. Continuous variables are summarized with the mean, standard deviation, median, and interquartile range. The chi-square test was used to examine the associations across categorical variables. Student's t-test was used to compare the RV parameters between groups with or without RV failure. The diagnostic performance of the test was evaluated through sensitivity and specificity analyses with the receiver operating characteristic (ROC) curve, thus aiding in determination of the optimal cutoff value. The correlation between dependent and independent parameters was examined with bivariate correlation and illustrated with a simple scatterplot. A P-value of 0.05 was considered statistically significant, whereas a P-value < 0.001 was considered highly significant. Confidence intervals were calculated at the 95% level.

Results

Table 1 shows the demographic characteristics of the study participants. The median age of children with rTOF for diagnosis of RV function was 9 (interquartile range 6−

Table 1: Characteristics of participating children by the presence or absence of RVF.

Children	Number = 150 (%)	Right ventricular failure (n = 24)%	No right ventricular failure (n = 126)%	P-value
Sex				
Male	75 (50)	8 (33.3)	67 (53.2)	0.06
Female	75 (50)	16 (66.7)	59 (48.8)	
Residence				
Inside city	104 (69.3)	11 (55)	93 (71.5)	
Outside city	46 (30.7)	9 (45)	37 (28.5)	0.1
Age				
3−6 years	36 (24)	1 (4.2)	35 (27.8)	
7−9 years	54 (36)	7 (29.2)	47 (37.3)	0.006*
≥10 years	60 (40)	16 (66.8)	44 (34.9)	
Weight				
≤20 kg	33 (22)	1 (4.1)	32 (25.4)	
21−30 kg	57 (38)	7 (29.2)	50 (39.7)	0.007*
≥31 kg	60 (40)	16 (66.7)	44 (34.9)	
Education				
Kindergarten	21 (14.0)	0 (0.0)	21 (16.7)	
Primary	108 (72)	20 (83.3)	88 (69.8)	0.01*
Secondary	21 (14.0)	4 (16.7)	17 (13.5)	

*refers to signifigant P value.

Table 2: Comparison of echo parameters for children with or without RVF.

Parameters	RV dysfunction, mean ± SD	Normal RV function, mean ± SD	t	P-value
TAPSE >1.7 cm	1.3 ± 0.11	1.9 ± 0.24	12.11	<0.001*
EF > 45%	35.5 ± 6.72	62.5 ± 7.81	14.58	<0.001*
RVESV 10−44 ml	69.8 ± 15.13	23.7 ± 10.83	−16.73	<0.001*
RVEDV 32−87 ml	110.1 ± 14.13	52.29 ± 16.42	−14.90	<0.001*
MPI <0.40	0.60 ± 0.12	0.21 ± 0.07	−19.30	<0.001*
Pmax mmHg	52.4 ± 14.08	14.9 ± 4.49	−23.71	<0.001*
Regional peak strain (%)				
Base lateral strain (BLS)	−12.7 ± 3.6	−21.4 ± 4.8	8.7	<0.001*
Mid lateral strain (MLS)	−10.2 ± 2.4	−16.7 ± 2.5	6.5	<0.001*
Apex lateral strain (ALS)	−9.1 ± 2.5	−18.9 ± 3.0	5.3	<0.001*
Regional peak strain rate (1/sec)				
Base lateral strain rate (BLSR)	−1.1 ± 0.5	−2.0 ± 1.0	0.9	<0.001*
Mid lateral strain rate (MLSR)	−0.9 ± 0.5	−1.7 ± 0.6	0.8	<0.001*
Apex lateral strain rate (ALSR)	−0.9 ± 0.5	−1.9 ± 0.7	0.9	<0.001*
Longitudinal RV strain (%)	−12.1 ± 2.3	−18.9 ± 1.8	6.9	<0.001*
Longitudinal RV strain rate (1/sec)	−0.9 ± 0.3	−1.9 ± 0.5	0.9	<0.001*

*refers to signifigant P value.

11) years, with a range of 3−13 years. Participants were frequency-matched by sex (50%). Sixteen girls (66.7%) had RVF and 59 (48.8%) had no RVF, whereas 8 boys (33.3%) had RVF and 67 (53.2%) no RVF, with P = 0.06. Of 150 children, 95.9% of children 7−9 years of age or older had abnormal RVF, whereas 72.2% of the same age group had normal RV function, with P = 0.006. The children's weight ranged from 12 to 50 kg (mean 27.6 ± SD 8.8 kg). The weights of the children in the two groups significantly differed (P = 0.007). Most children diagnosed with RV failure (83.3%) were in primary school, whereas most children with normal right ventricles (69.8%) were in secondary school (P = 0.01).

Table 2 compares the mean ECG and TDI parameter values for children with rTOF, with versus without RVF. TAPSE was significantly lower in children with than without RVF; the mean TAPSE was 1.3 ± 0.11 cm vs. 1.9 ± 0.24 cm, respectively ($P \leq 0.001$). Children with RVF had a lower RVEF% than those with normal RV function. The mean EF was 35.5 ± 6.72 and 62.5 ± 7.81,

Table 3: Comparison of sensitivity and specificity between conventional and ST echo.

Type	N	Sensitivity	Specificity	PPV	NPV	Accuracy
Conventional echo	20 (13%)	83.3%	100%	100%	96.9%	97.3%
Speckle tracking echo	24 (16%)	100%	96.9%	83.3%	100%	97.3%

respectively (P ≤ 0.001). Significantly higher mean values of RVESV (69.8 ± 15.13) and RVEDV (110.1 ± 14.13 ml) were observed in children diagnosed with RVF than in children without RVF (RVESV 23.7 ± 10.83 and RVEDV 52.29 ± 16.42 ml; P ≤ 0.001 for both). Children with normal RV function showed a smaller mean MPI (0.21 ± 0.07), whereas those with RVF showed a significantly higher mean MPI (0.60 ± 0.12), with a Pmax of 52.4 ± 14.08 vs. 14.9 ± 4.49 mm/Hg (P < 0.001).

In addition, the strain of RVF and non-RVF of the three segmental lateral RV walls was as follows: BLS: −12.7 ± 3.6 vs. −21.4 ± 4.8, P < 0.001, respectively; MLS: −10.2 ± 2.4 vs. −16.7 ± 2.5, P < 0.001, respectively; and ALS: −9.1 ± 2.5 vs. −18.9 ± 3.0, P < 0.001, respectively. The strain rate values of RVF and non-RVF were as follows: BLSR: −1.1 ± 0.5 vs. −2.0 ± 1.0, P < 0.001, respectively; MLSR: −0.9 ± 0.5 vs. −1.7 ± 0.6, P < 0.001, respectively; and ALSR: −0.9 ± 0.5 vs. −1.9 ± 0.7, P < 0.001, respectively. The RV wall's longitudinal ST and SR values significantly differed between groups (P < 0.001). Lower longitudinal ST and SR (−12.1 ± 2.3 and −0.9 ± 0.3) were observed in children with RVF than children who did not develop RVF (−18.9 ± 1.8 and −1.9 ± 0.5; P ≤ 0.001).

The study was aimed at evaluating and comparing the sensitivity and specificity of two ECG techniques, conventional and speckle tracking ECG, for RVF detection. Conventional ECG had 83.3% sensitivity and 100% specificity, with a 100% positive predictive value and 96.9% negative predictive value. In contrast, speckle tracking analysis exhibited a sensitivity of 100% and a specificity of 96.9%; a positive predictive value of 83.3% and a negative predictive value of 100%; and an accuracy of 97.3% for both. Regarding the application of conventional ECG (2D echo), among the 150 children assessed, only 20 (13%) were diagnosed with RVF. However, with the use of advanced ECG ST and SR, 24 children were identified as having RVF, corresponding to a proportion of 16% (Table 3).

ROC curve analyses were performed to evaluate the clinical effectiveness of various parameters in diagnosing RVF, according to the criteria of RVEF < 45% and TAPSE < 1.7 cm, measured by 2D ECG. Sensitivity and specificity values and their corresponding optimal cutoff values were

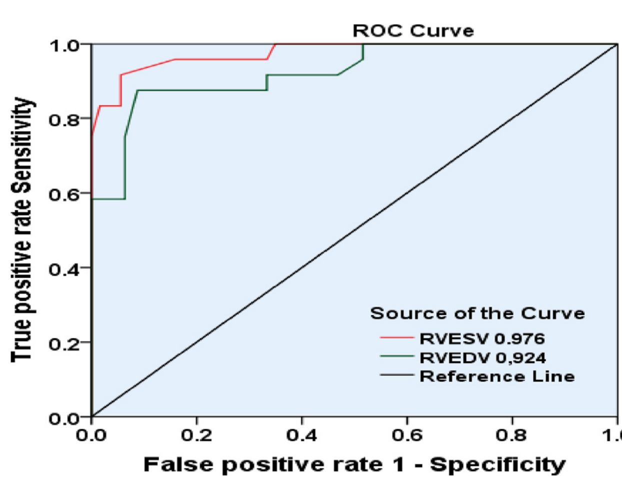

Figure 1: Receiver operating characteristic for a conventional echo of diagnosis of RV.

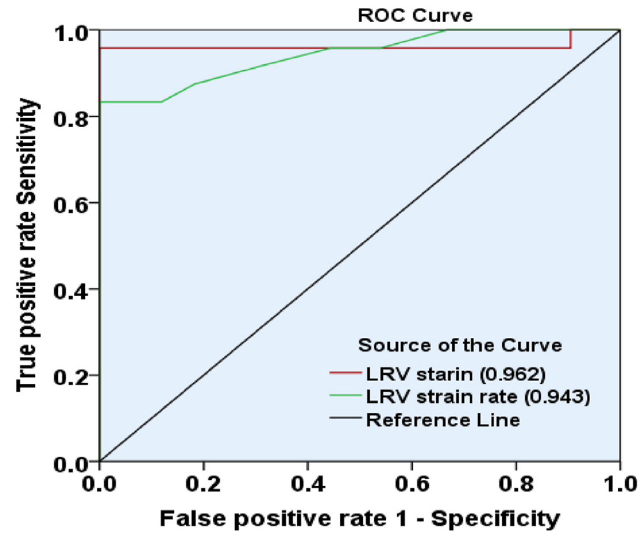

Figure 2: Receiver operating characteristic for strain and strain rate of diagnosis of RVF.

determined. Figure 1 displays the outcomes of these analyses, illustrating the optimal cutoff value for RVESV at 31.5 ml. A sensitivity of 91.7% and specificity of 94.4% were achieved, with an area under the curve (AUC) of 0.976 (p < 0.001). Additionally, the cutoff value of RVEDV was determined to be 73.5 ml, thus yielding a sensitivity of 87.5% and specificity of 87%, and an AUC of 0.924 (p < 0.001). These findings demonstrated the robust discriminatory capacity of these parameters in accurately diagnosing RVF, through effectively distinguishing between patients with RVF and healthy individuals with normal RV function.

We used ROC curve analysis to evaluate the efficacy of ST echo parameters, specifically LRVS and LRVSR, in diagnosing RVF in rTOF. Figure 2 shows the ROC curve, representing the relationship between sensitivity and specificity. For the diagnosis of RVF, the optimal cut-off value for LRVS was determined to be −15.8%. The AUC was computed to be 0.962 (P < 0.001), thus indicating a high discriminatory capacity. This parameter exhibited a sensitivity of 95.8% and specificity of 95.2%, thereby providing valuable diagnostic accuracy.

Regarding LRVSR, the best cut-off value was determined to be −1.5 s. The sensitivity was 87.5%, and the specificity was 81.7%. The AUC was calculated as 0.943 (P < 0.001), thus highlighting favorable diagnostic performance in identifying RVF in children with rTOF. These findings suggested that both LRVS and LRVSR may be promising tools for non-intrusive diagnosis of RVF in this specific patient population.

Figure 3 shows the scatter plot analysis, indicating significant correlations between LRVS and various echo parameters. A positive association was observed between LRVS and TAPSE (r = 0.656, P < 0.001) and EF (r = 0.675, P < 0.001). In contrast, LRVS exhibited negative correlations with RVEDV (r = −0.684, P < 0.001) and RVESV (r = −0.718, P < 0.001).

Table 4 shows the correlation of LRVSR with RV function in children with postoperative TOF with absolute echo parameters. A weak positive correlation of LRVSR with TAPSE (r = 0.465, P ≤ 0.001) and EF (r = 0.443, P ≤ 0.001) was observed. Moreover, a weak inverse correlation was

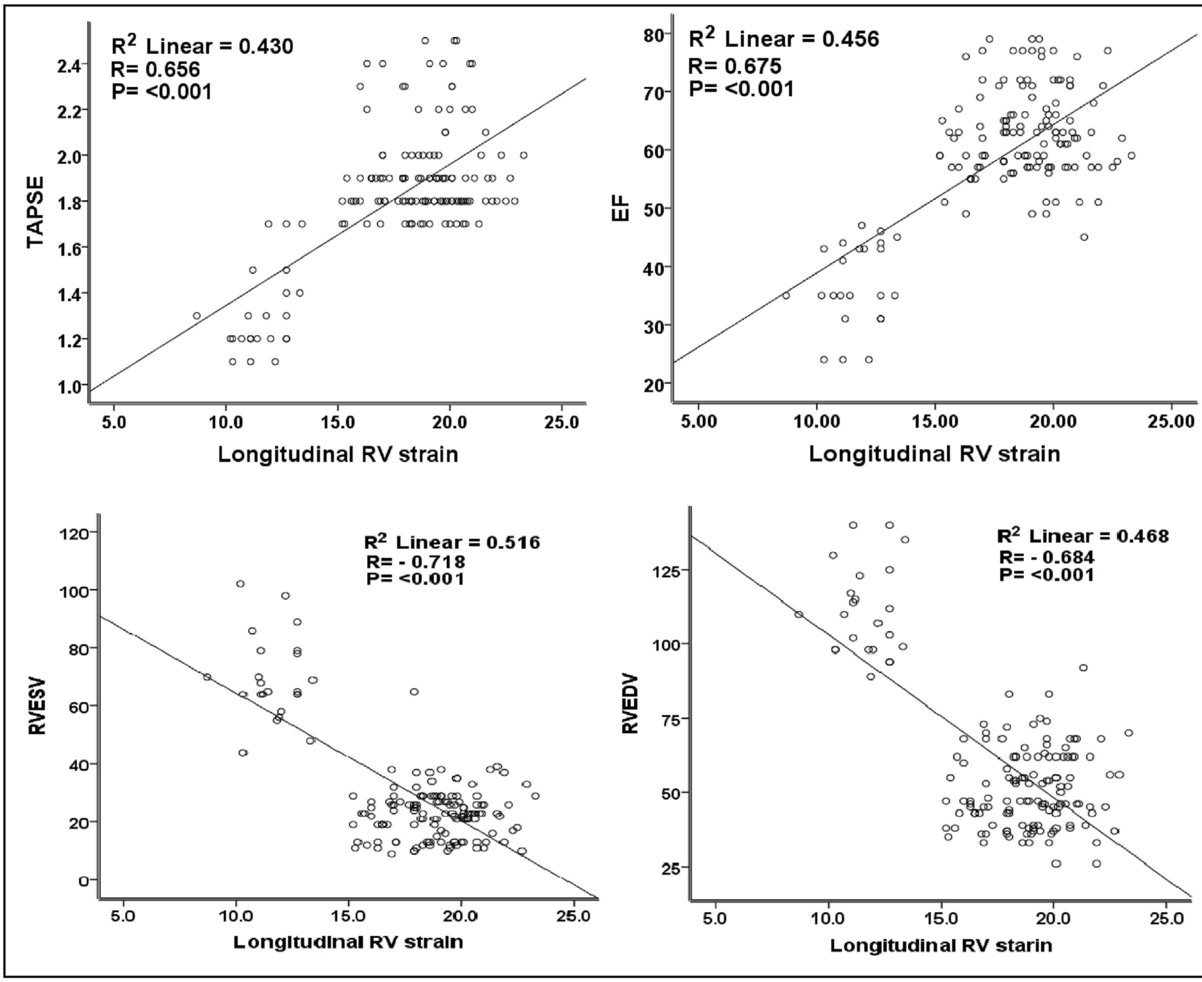

Figure 3: Correlation of LRVS with conventional echo parameters.

Table 4: Correlation of LRVSR with absolute ECG parameters.

Parameters	Pearson's r	P-value
TAPSE	0.465	<0.001*
EF	0.443	<0.001*
RVESV	−0.455	<0.001*
RVEDV	−0.459	<0.001*
MPI	−0.526	<0.001*
Pmax	−0.491	<0.001*

*refers to signifigant P value.

observed between LRVSR and the following echo parameters: RVESV (r = −0.455, P ≤ 0.001), RVEDV (r = −0.459, P ≤ 0,001), IMP (r = −0.526, P ≤ 0.0010), and Pmax (r = −0.491, P ≤ 0.001).

Figure 4 demonstrates the application of standard ECG and speckle tracking parameters for assessing right ventricular function in children who have undergone surgical repair for tetralogy of Fallot (TOF). Panel **A** uses Simpson's method to measure volumetric parameters, including the ejection fraction (EF), thus providing a quantitative assessment of ventricular function. Panel **B** introduces tricuspid annular plane systolic excursion (TAPSE) as a tool for detecting right ventricular failure (RVF) in this patient group, with abnormal TAPSE and EF values indicating the presence of RVF. Panels **C** and **D** present a novel diagnostic technique, speckle tracking echo, which uses strain and strain rate measurements to evaluate systolic myocardial function. This innovative approach offers valuable insights into assessing right ventricular function in children who have undergone surgical repair for TOF.

Table 5 presents ECG parameters as T-WD, P-WD, and QRS duration. The ECG showed a wide P-WD with a mean of 101 ± 41.66 ms for children with RV failure, whereas children with normal RV function showed a narrowed P-WD with a mean of 77.08 ± 14.09 ms (P ≤ 0.001). The T-WD values were near 0, thus indicating increased dispersion in children with RVF, with a mean of 0.77 ± 0.16 ms, whereas in children without RVF, T-WD values close to 1 indicated a decrease in dispersion (mean 0.88 ± 0.16 ms; P ≤ 0.009). Prolonged QRS duration was observed in children with RVF, with a mean of

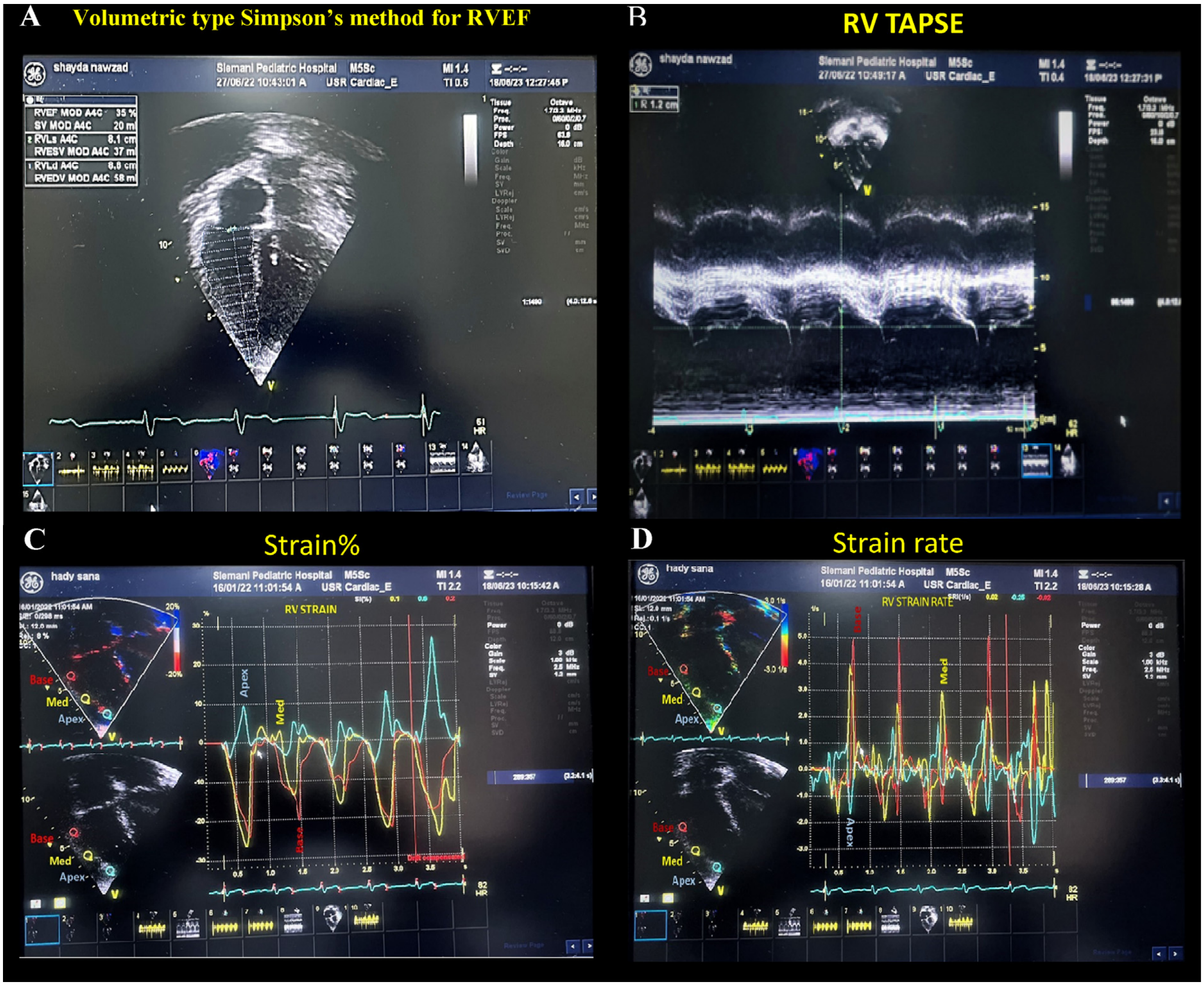

Figure 4: Conventional ECG and speckle tracking for diagnosis of RV.

Table 5: Electrocardiography measurements in children with or without RVF.

ECG parameters/ms	Abnormal RV function, mean ± SD	Normal RV function, mean ± SD	t	P-value
P -WD	101 ± 41.66	77.08 ± 14.09	−5.01	<0.001
T-WD (V4 through V6)	0.77 ± 012	0.88 ± 0.16	2.64	0.009
QRS duration	132.5 ± 18.88	81.77 ± 14.16	−19.95	<0.001

132.5 ± 18.88 ms, whereas children without RVF had a shorter mean QRS duration of 81.77 ± 14.16 ms ($P \leq 0.001$).

Discussion

To our knowledge, this is the first study using advanced speckle-tracking ECG strain and strain rate to diagnose RVF in children with complete TOF correction in Iraq. Our study was performed to determine the sensitivity and specificity of speckle tracking echo in investigation of RVF. Notably, advanced speckle-tracking ECG was more sensitive than conventional ECG and was able to discriminate patients with RVF, particularly those with asymptomatic heart failure, from those without RVF. The findings of our study are consistent with those from two previous studies.[26,27] According to the literature, the RV's distinct crescent shape precludes precise quantification of its size and function with conventional echo.[28] Conventional echocardiographic evaluation of the RV remains challenging, particularly in children with rTOF, because of RV hypertrophy. Hence, acquiring established echocardiographic parameters for assessing global RV function can be challenging and may not always yield accurate results. Our hypothesis aligns with the findings of the two studies described above.[29,30]

Notably, TAPSE and EF measurements are widely recognized to be highly reproducible and reliable in the investigation of RV function. These parameters have demonstrated high specificity in detecting RV systolic dysfunction in heart failure cases.[31] Furthermore, on the basis of two studies that used TAPSE and EF to determine systolic RVF by conventional ECG, we defined systolic RVF as TAPSE <1.7 cm and EF 45%.[32,33] Accordingly, we focused on the TAPSE and EF for diagnosing RVF by conventional ECG. We found that children with than without RVF had a lower TAPSE of 1.7 cm and EF of less than 45%. Notably, a decrease in TAPSE led to a decrease in RVEF. A study by Rydman et al.[34] corroborates our findings and aligns with previous research indicating a progressive decline in TAPSE in cases with postoperative TOF and RVF.[35,36] Another notable finding was that EF, as measured with the Simpson method, was an independent predictor of RVF. We observed that children who developed RVF had a significantly lower EF (below 45%) than children without RVF. Our findings are consistent with those from a previous study.[37] Furthermore, the Tei index, also referred to as the myocardial performance index, serves as a valuable quantitative measure for assessing the myocardium's systolic and diastolic function. It is particularly useful in evaluating RV function in patients with RVF and pulmonary arterial hypertension. Conventional echo performed on children with rTOF revealed that children with RVF had an abnormal MPI, which was significantly higher than that in children who did not develop RVF. Our results are consistent with those from a previous study.[38]

We analyzed RVESV and RVEDV in children with post-TOF to derive normal predicted values in each patient, because of the lack of absolute echo parameters predicting normal RVESV and RVEDV in children with rTOF. RVESV and RVEDV were measured with 2D echo according to Simpson's biplane rules, and the RV cardiac volume was markedly increased. All children with postoperative TOF diagnosed with RV failure had elevated RVESV and RVEDV volume. Our results were consistent with those from two previous studies.[39,40] We hypothesize that pulmonary stenosis and regurgitation might cause the RV chamber to dilate and impair systolic function, thus increasing RVESV. As the RVESV increases, the RVEF and TAPSE decrease and might serve as a good indicator for the need for pulmonary valve replacement.

The literature has importantly revealed that patients with rTOF with severe pulmonary regurgitation are at elevated risk of developing RV dilatation and eventually failure.[41] TDI was used to measure the pulmonary gradients, and the pulmonary artery gradient was higher in children who developed RVF than in children who did not. Bouzas et al. (38) have reported the same study finding. Yoo et al., in 2012, also reported that children with rTOF remain at risk of PR and PS and RVF have a higher pulmonary gradient and mean pulmonary gradient than children without RVF.[42]

ROC analyses demonstrated that RVESV and RVEDV had good sensitivity and specificity in predicting RV dysfunction, in agreement with the results of two previous studies.[43,44]

Advanced ECG technologies have been proposed to enable quantitative assessment of regional myocardial function and deformities. The current study focused on children with TOF correction with STI, to provide an alternative method for measuring RV function. On the basis of a literature review, strain was defined as the percentage change in myocardial deformation, and its derivative, SR, was defined as the myocardium's deformation rate (speed of deformation) over time.[45] We discovered that use of advanced speckle tracking echoes, ST, and SR for the investigation of RVF might enable more sensitive detection and accurate RV parameters. This finding is compatible with those from a previous study.[46] Several studies have documented that the mean longitudinal strain (LS) and longitudinal strain rate (LSR) of the RV-free wall, particularly in the basal, middle, and apical segments, and an absolute systolic strain rate below 20%, indicate cardiovascular events.[47–49]

In our study, for calculating the LS and LSR, we determined the RV endocardium and myocardium, and we selected three regions: basal, middle, and apex. The speckle tracking echo examination of the children with rTOF indicated that the LRV-free wall ST and SR at the basal, middle, and apical levels were significantly lower in children with RVF than in children with normal RV function. Interestingly, the LRVS was significantly lower (mean of -12 ± 2.3) in children diagnosed with RVF than children with normal RV function (mean of -18.9 ± 1.8; $P \leq 0.001$). Our findings were similar to those of two studies on TOF children conducted in China.[37,50] LST and LSR, measured by Doppler tissue imaging and 2D speckle tracking echo, are more reliable and accurate than conventional 2D and TDI in measuring RV systolic deformation and detecting regional myocardial deformation and impaired speed velocity. Our interpretation is consistent with the results of a prior study[51] reporting a strong correlation between LRVS and LRVSR with RV echo parameters. We observed that increased LRVS and LRVSR were associated with increased TAPSE and RVEF, and decreased LRVS and LRVSR were also associated with decreased RVEF and TAPSE, in agreement with previous studies.[50,52] One possible explanation for these findings is that LRVS and LRVSR reflect RV contractile function. Increasing LRVS and LRVSR indicate better myocardial contractility and deformation, and improving TAPSE and RVEF. In contrast, decreased LRVS and LRVSR may suggest impaired contractility and diminished deformation, thus resulting in decreased TAPSE and RVEF. Furthermore, we observed a correlation of LRVS and LRVSR with all 2D ECG parameters, such as RVEDV and RVEDV, in agreement with prior studies.[53,54] One possible interpretation is that as LRVS and LRVSR decrease, RVEDV and RVESV tend to increase. This finding may indicate impaired RV function, because decreased strain and strain rates suggest diminished myocardial contractility and deformation. Consequently, the ventricular chambers may dilate during diastole (RVEDV) and fail to contract effectively during systole (RVESV), thus resulting in increased volumes. Overall, children with rTOF diagnosed with RVF had lower ECG parameters, and strain and strain rate values, than children who did not develop RVF. Our study indicated that children who developed RVF had significantly higher P-WD and longer QRS duration than children with normal RV function. These results are consistent with those from two previous studies.[55–57] The explanation might be associated with the changes in cardiac electrophysiology due to the underlying structural abnormalities and surgical intervention, and dilated atria and ventricles. rTOF often involves RV outflow tract reconstruction, which may lead to scarring or fibrosis, thereby causing electrical conduction abnormalities and increasing the risk of arrhythmias. Right atrial dilation and dysfunction can also contribute to conduction abnormalities and arrhythmias. These changes can increase P-WD and QRS duration, and may potentially indicate the presence of ventricular arrhythmias and the risk of sudden death. Another notable finding in this study was that the T-wave represents ventricular myocardium repolarization, and T-WD may be the best marker for diagnosing RVF. Children diagnosed with than without RVF had significantly lower T-WD, thus reflecting greater repolarization heterogeneity. The findings of Tikkanen et al. are consistent with our results.[58] The explanation for these findings may be associated with RV dysfunction leading to changes in ventricular repolarization.

Conclusions

In conclusion, speckle tracking is a novel and sophisticated method to investigate RV dysfunction in patients with rTOF. It is a low-risk, non-invasive technique for patients with rTOF that enables accurate diagnosis of RV myocardial function and velocity. Our findings underscore the insufficiency of conventional echocardiographic parameters, which focus on RV volume rather than myocardial motion, in accurately evaluating RV function in patients with total TOF correction. In contrast, speckle tracking is a valuable ECG technique to accurately measure and assess global RV function and myocardial velocity in patients with TOF. Furthermore, this new technique may provide additional information not obtained by conventional ECG parameters, and provide a better mechanism for RVF diagnosis in rTOF patients. We also discovered an increase in RV volume in children with rTOF caused by pulmonary stenosis. Increases in non-volumetric parameters such as RVEF and TAPSE were negatively correlated with increases in other RV volume parameters. Children with RVF have markedly elevated volumetric parameters such as RVESV, RVEDV, and P max. Early diagnosis of RV failure aids in decision-making regarding whether pulmonary valve replacement is necessary for prolonged survival of children with rTOF.

Strengths and limitations

The primary strength of the study is that this it is the first, to our knowledge, to investigate RV failure in children with complete rTOF in Iraq, by using a new advanced echo technique known as speckle tracking. This study has several limitations. One limitation of transthoracic ECG is the lack of standard reference values for RV ECG parameters, particularly in children with rTOF. Furthermore, with rTOF, a significantly dilated RV may restrict the collection of excellent 2D parameters. Speckle-tracking ECG based on examining the longitudinal RV-free wall may result in the misdiagnosis of myocardial septal deformities. The lack of an absolute reference strain and strain rate for examination of the accuracy of our measures might be viewed as a limitation of our investigation; this study relied on an adult reference, and only prospective outcome studies can evaluate the clinical relevance of our approach. Speckle tracking ECG also has certain limitations that should be considered, including the requirement for a precise frame rate, potential difficulties in accurately delineating the epicardial and endocardial borders in low-quality images, the need for expertise in using analysis software, and the limited availability of software specifically designed for analyzing the intricate geometry of the right ventricle.

Source of funding

This research received no specific grant from funding agencies in the public, commercial, or not-for-profit sectors.

Conflict of interest

The authors have no conflict of interest to declare

Ethical approval

This study was approved by the scientific and ethics committees of the College of Medicine, University of Sulaimani, Sulaymaniyah, Iraq (No. 80-UoS on May 5, 2021). All procedures in this study complied with the Declaration of Helsinki. The patient/parents filled out a consent form, and families were informed of the purpose of the study. In addition, they were allowed to withdraw from the study at any time without providing a reasonable declaration.

Authors contributions

The authors' contributions to the article are as follows: NK designed the study, collected the data, performed the statistical analysis, wrote the results and methods sections, and performed ECG. AS performed echo for both conventional and advancing speckle tracking, wrote the discussion section, revised the language of the article, and provided critical feedback. BM wrote the conclusion and abstract, revised the article's scientific content, provided valuable input, and approved the final text. All authors have critically reviewed and approved the final draft and are responsible for the content and similarity index of the manuscript.

Acknowledgment

The authors acknowledge and thank the staff at Sulaimani Children's Heart Hospital, the participating patients, and the Department of Family Community Medicine for their invaluable support and contributions to the successful completion of this study.

References

1. Hoffman JI, Kaplan S. The incidence of congenital heart disease. **J Am Coll Cardiol 2002**; 39(12): 1890−1900.
2. Van Praagh R. The first Stella van Praagh memorial lecture: the history and anatomy of tetralogy of Fallot. In: *Seminars in thoracic and cardiovascular surgery pediatric cardiac surgery annual*; 2009. pp. 19−38.
3. Anderson RH, Baker EJ, Redington A, Rigby ML, Penny D, Wernovsky G. *Paediatric cardiology*. Elsevier Health Sciences; 2009.

4. Poon LC, Huggon IC, Zidere V, Allan LD. Tetralogy of Fallot in the fetus in the current era. **Ultrasound Obstet Gynecol: Off J Int Soc Ultrasound Obstet Gynecol 2007**; 29(6): 625−627.
5. Chew C, Halliday JL, Riley MM, Penny DJ. Population-based study of antenatal detection of congenital heart disease by ultrasound examination. **Ultrasound Obstet Gynecol: Off J Int Soc Ultrasound Obstet Gynecol 2007**; 29(6): 619−624.
6. Gatzoulis MA, Till JA, Somerville J, Redington A. QRS prolongation relates to right ventricular size and predicts malignant ventricular arrhythmias and sudden death. **Circulation 1995**; 92(2): 231−237.
7. Marwick TH. The role of echocardiography in heart failure. **J Nucl Med 2015**; 56(Supplement 4): 31S−38S.
8. Dufendach KA, Zhu T, Diaz Castrillon C, Hong Y, Countouris ME, Hickey G, et al. Pre-implant right ventricular free wall strain predicts post-LVAD right heart failure. **J Card Surg 2021**; 36(6): 1996−2003.
9. Vizzardi E, Bonadei I, Sciatti E, Pezzali N, Farina D, D'Aloia A, et al. Quantitative analysis of right ventricular (RV) function with echocardiography in chronic heart failure with no or mild RV dysfunction: comparison with cardiac magnetic resonance imaging. **J Ultrasound Med 2015**; 34(2): 247−255.
10. Henein MY, O'Sullivan CA, Coats AJ, Gibson DG. Angiotensin-converting enzyme (ACE) inhibitors revert abnormal right ventricular filling in patients with restrictive left ventricular disease. **J Am Coll Cardiol 1998**; 32(5): 1187−1193.
11. Gorter TM, van Veldhuisen DJ, Bauersachs J, Borlaug BA, Celutkiene J, Coats AJ, et al. Right heart dysfunction and failure in heart failure with preserved ejection fraction: mechanisms and management. Position statement on behalf of the Heart Failure Association of the European Society of Cardiology. **Eur J Heart Fail 2018**; 20(1): 16−37.
12. Edvardsen T, Klaeboe LG. Imaging and heart failure: myocardial strain. **Curr Opin Cardiol 2019**; 34(5): 490−494.
13. Saha SK, Kiotsekoglou A, Gopal AS, Lindqvist P. Biatrial and right ventricular deformation imaging: implications of the recent EACVI consensus document in the clinics and beyond. **Echocardiography (Mount Kisco, NY) 2019**; 36(10): 1910−1918.
14. Smith BC, Dobson G, Dawson D, Charalampopoulos A, Grapsa J, Nihoyannopoulos P. Three-dimensional speckle tracking of the right ventricle: toward optimal quantification of right ventricular dysfunction in pulmonary hypertension. **J Am Coll Cardiol 2014**; 64(1): 41−51.
15. Amsallem M, Mercier O, Kobayashi Y, Moneghetti K, Haddad F. Forgotten No more: a focused update on the right ventricle in cardiovascular disease. **JACC Heart failure 2018**; 6(11): 891−903.
16. Iacoviello M, Citarelli G, Antoncecchi V, Romito R, Monitillo F, Leone M, et al. Right ventricular longitudinal strain measures independently predict chronic heart failure mortality. **Echocardiography (Mount Kisco, NY) 2016**; 33(7): 992−1000.
17. Jamal F, Bergerot C, Argaud L, Loufouat J, Ovize M. Longitudinal strain quantitates regional right ventricular contractile function. **Am J Physiol Heart Circ Physiol 2003**; 285(6): H2842−H2847.
18. Leitman M, Lysyansky P, Sidenko S, Shir V, Peleg E, Binenbaum M, et al. Two-dimensional strain−a novel software for real-time quantitative echocardiographic assessment of myocardial function. **J Am Soc Echocardiogr 2004**; 17(10): 1021−1029.
19. Monaco M, Williams I. Tetralogy of Fallot: fetal diagnosis to surgical correction. **Minerva Pediatr 2012**; 64(5): 461−470.
20. Tanasan A, Kocharian A, Zanjani KS, Payravian FK, Torabian S. Correlation between QRS duration, pulmonary insufficiency and right ventricle performance in totally corrected tetralogy of Fallot. **Iran J Pediatr 2013**; 23(5): 593−596.
21. Dilaveris PE, Gialafos EJ, Andrikopoulos GK, Richter DJ, Papanikolaou V, Poralis K, et al. Clinical and electrocardiographic predictors of recurrent atrial fibrillation. **Pacing Clin Electrophysiol: PACE 2000**; 23(3): 352−358.
22. Rudski LG, Lai WW, Afilalo J, Hua L, Handschumacher MD, Chandrasekaran K, et al. Guidelines for the echocardiographic assessment of the right heart in adults: a report from the American Society of Echocardiography: endorsed by the European Association of Echocardiography, a registered branch of the European Society of Cardiology, and the Canadian Society of Echocardiography. **J Am Soc Echocardiogr 2010**; 23(7): 685−713.
23. Focardi M, Cameli M, Carbone SF, Massoni A, De Vito R, Lisi M, et al. Traditional and innovative echocardiographic parameters for the analysis of right ventricular performance in comparison with cardiac magnetic resonance. **Eur Heart J Cardiovasc Imaging 2015**; 16(1): 47−52.
24. Prihadi EA, van der Bijl P, Dietz M, Abou R, Vollema EM, Marsan NA, et al. Prognostic implications of right ventricular free wall longitudinal strain in patients with significant functional tricuspid regurgitation. **Circ Cardiovasc Imaging 2019**; 12(3):e008666.
25. Wang TKM, Grimm RA, Rodriguez LL, Collier P, Griffin BP, Popović ZB. Defining the reference range for right ventricular systolic strain by echocardiography in healthy subjects: a meta-analysis. **PLoS One 2021**; 16(8):e0256547.
26. Lemarié J, Maigrat C-H, Kimmoun A, Dumont N, Bollaert P-E, Selton-Suty C, et al. Feasibility, reproducibility and diagnostic usefulness of right ventricular strain by 2-dimensional speckle-tracking echocardiography in ARDS patients: the ARD strain study. **Ann Intensive Care 2020**; 10(1): 1−10.
27. Pastore MC, Mandoli GE, Contorni F, Cavigli L, Focardi M, D'Ascenzi F, et al. Speckle tracking echocardiography: early predictor of diagnosis and prognosis in coronary artery disease. **BioMed Res Int 2021**; 2021.
28. Mauger C, Gilbert K, Lee AM, Sanghvi MM, Aung N, Fung K, et al. Right ventricular shape and function: cardiovascular magnetic resonance reference morphology and biventricular risk factor morphometrics in UK Biobank. **J Cardiovasc Magn Reson 2019**; 21(1): 1−13.
29. Orde S, Slama M, Hilton A, Yastrebov K, McLean A. Pearls and pitfalls in comprehensive critical care echocardiography. **Crit Care 2017**; 21(1): 1−10.
30. Wu VC, Takeuchi M. Echocardiographic assessment of right ventricular systolic function. **Cardiovasc Diagn Ther 2018**; 8(1): 70−79.
31. Lu CW, Chen YS, Wang MJ. Role of intraoperative transesophageal echocardiography for diagnosing and managing pulmonary embolism in the perioperative period. **Anesth Analg 2005**; 100(1): 293.
32. Kossaify A. Echocardiographic assessment of the right ventricle, from the conventional approach to speckle tracking and three-dimensional imaging, and insights into the "right way" to explore the forgotten chamber. **Clin Med Insights Cardiol 2015**; 9: 65−75.
33. Greutmann M, Ruperti J, Schwitz F, Haag N, Lopes BS, Meier L, et al. High variability of right ventricular volumes and function in adults with severe pulmonary regurgitation late after tetralogy of Fallot repair. **Am J Cardiol 2022**; 166: 88−96.
34. Rydman R, Larsen F, Caidahl K, Alam M. Right ventricular function in patients with pulmonary embolism: early and late findings using Doppler tissue imaging. **J Am Soc Echocardiogr: Off Publ Am Soc Echocardiogr 2010**; 23(5): 531−537.
35. López-Candales A, Rajagopalan N, Saxena N, Gulyasy B, Edelman K, Bazaz R. Right ventricular systolic function is not the sole determinant of tricuspid annular motion. **Am J Cardiol 2006**; 98(7): 973−977.

36. Koestenberger M, Nagel B, Ravekes W, Everett AD, Stueger HP, Heinzl B, et al. Tricuspid annular plane systolic excursion and right ventricular ejection fraction in pediatric and adolescent patients with tetralogy of Fallot, patients with atrial septal defect, and age-matched normal subjects. **Clin Res Cardiol: Off J German Cardiac Soc 2011**; 100(1): 67–75.
37. Li JY, Li RJ, Ma N, Wang FY, Zhang XL, Xie JJ, et al. Assessment of right ventricular strain in children with repaired tetralogy of Fallot using speckle tracking imaging. **Chin Med J 2019**; 132(6): 744–748.
38. Tei C, Dujardin KS, Hodge DO, Bailey KR, McGoon MD, Tajik AJ, et al. Doppler echocardiographic index for assessment of global right ventricular function. **J Am Soc Echocardiogr: Off Publ Am Soc Echocardiogr 1996**; 9(6): 838–847.
39. Chronic testosterone treatment in men with coronary artery disease: a study with perfusion cardiovascular magnetic resonance. In: Elkington A, Webb C, Gatehouse P, Firmin D, Pennell D, Collins P, editors. *Circulation*. Two Commerce Sq, 2001 Market St, Philadelphia: Lippincott Williams & Wilkins; 2004.
40. Bidviene J, Muraru D, Kovacs A, Lakatos B, Ereminiene E, Liptai C, et al. Global and regional right ventricular mechanics in repaired tetralogy of Fallot with chronic severe pulmonary regurgitation: a three-dimensional echocardiography study. **Cardiovasc Ultrasound 2021**; 19(1): 1–11.
41. Bouzas B, Kilner PJ, Gatzoulis MA. Pulmonary regurgitation: not a benign lesion. **Eur Heart J 2005**; 26(5): 433–439.
42. Yoo BW, Kim JO, Kim YJ, Choi JY, Park HK, Park YH, et al. Impact of pressure load caused by right ventricular outflow tract obstruction on right ventricular volume overload in patients with repaired tetralogy of Fallot. **J Thorac Cardiovasc Surg 2012**; 143(6): 1299–1304.
43. Zhang S, Yang ZG, Sun JY, Wen LY, Xu HY, Zhang G, et al. Assessing right ventricular function in patients with hypertrophic cardiomyopathy with cardiac MRI: correlation with the New York Heart Function Assessment (NYHA) classification. **PLoS One 2014**; 9(9):e104312.
44. Karim MR, Rahman MA, Mondol RU, Chowdhury TA, Ghose RK. Sensitivity and specificity of myocardial performance indexing assessing acute right ventricular infarction. **TAJ J Teach Assoc 2022**; 35(1): 17–24.
45. Duncan AE, Alfirevic A, Sessler DI, Popovic ZB, Thomas JD. Perioperative assessment of myocardial deformation. **Anesth Analg 2014**; 118(3): 525–544.
46. Jasaityte R, D'hooge J. Strain rate imaging: fundamental principles and progress so far. **Imag Med 2010**; 2(5): 547.
47. Motoji Y, Tanaka H, Fukuda Y, Ryo K, Emoto N, Kawai H, et al. Efficacy of right ventricular free-wall longitudinal speckle-tracking strain for predicting long-term outcome in patients with pulmonary hypertension. **Circ J: Off J Jpn Circ Soc 2013**; 77(3): 756–763.
48. Scherptong RW, Mollema SA, Blom NA, Kroft LJ, de Roos A, Vliegen HW, et al. Right ventricular peak systolic longitudinal strain is a sensitive marker for right ventricular deterioration in adult patients with tetralogy of Fallot. **Int J Cardiovasc Imag 2009**; 25(7): 669–676.
49. Hoit BD. Strain and strain rate echocardiography and coronary artery disease. **Circ Cardiovasc Imaging 2011**; 4(2): 179–190.
50. Li Y, Xie M, Wang X, Lu Q, Zhang L, Ren P. Impaired right and left ventricular function in asymptomatic children with repaired tetralogy of Fallot by two-dimensional speckle tracking echocardiography study. **Echocardiography (Mount Kisco, NY) 2015**; 32(1): 135–143.
51. Lu KJ, Chen JX, Profitis K, Kearney LG, DeSilva D, Smith G, et al. Right ventricular global longitudinal strain is an independent predictor of right ventricular function: a multimodality study of cardiac magnetic resonance imaging, real time three-dimensional echocardiography and speckle tracking echocardiography. **Echocardiography (Mount Kisco, NY) 2015**; 32(6): 966–974.
52. Bannehr M, Kahn U, Liebchen J, Okamoto M, Haehnel V, Georgi C, et al. Right ventricular longitudinal strain predicts survival in patients with functional tricuspid regurgitation. **Can J Cardiol 2021**; 37(7): 1086–1093.
53. Ji M, Wu W, He L, Gao L, Zhang Y, Lin Y, et al. Right ventricular longitudinal strain in patients with heart failure. **Diagnostics (Basel, Switzerland) 2022**; 12(2).
54. Vîjîiac A, Onciul S, Guzu C, Verinceanu V, Bătăilă V, Deaconu S, et al. The prognostic value of right ventricular longitudinal strain and 3D ejection fraction in patients with dilated cardiomyopathy. **Int J Cardiovasc Imag 2021**; 37(11): 3233–3244.
55. Hauser M, Eicken A, Kuehn A, Hess J, Fratz S, Ewert P, et al. Managing the right ventricular outflow tract for pulmonary regurgitation after tetralogy of Fallot repair. **Heart Asia 2013**; 5(1): 106–111.
56. Bassareo PP, Mercuro G. QRS complex enlargement as a predictor of ventricular arrhythmias in patients affected by surgically treated tetralogy of Fallot: a comprehensive literature review and historical overview. **ISRN Cardiol 2013**; 2013: 782508.
57. Salih AF, Brazinji AFA. Value of P wave dispersion in pediatric patients with secundum atrial septal defect. **Electron J Gen Med 2019**; 16(6).
58. Tikkanen JT, Kenttä T, Porthan K, Huikuri HV, Junttila MJ. Electrocardiographic T wave abnormalities and the risk of sudden cardiac death: the Finnish perspective. **Ann Noninvasive Electrocardiol: Off J Int Soc Holter Noninvasive Electrocardiol 2015**; 20(6): 526–533.

How to cite this article: Kamal NM, Salih AF, Ali BM. Speckle tracking echocardiography for diagnosis of right ventricular failure in children with totally corrected tetralogy of Fallot in Sulaimani, Iraq. J Taibah Univ Med Sc 2024;19(1):198–208.